Gyrofluid simulations on the effects of resonant magnetic perturbations on ideal ballooning unstable H-mode states

J. Peer[1], A. Kendl[1], T. T. Ribeiro[2]

[1] *Institute for Ion Physics and Applied Physics, University of Innsbruck, Association Euratom-ÖAW, A-6020 Innsbruck, Austria*

[2] *Max-Planck-Institute for Plasma Physics, Euratom Association, D-85748 Garching, Germany*

Introduction

The external application of resonant magnetic perturbations (RMPs) on tokamak edge plasmas allows to control and mitigate edge localized modes (ELMs) [1]. In this study, we employ the gyrofluid model GEMR to investigate the effects of RMPs on ideal ballooning ELMs. Moreover, we address the RMP induced suppression of repetitive transport bursts in H-mode-like states including an artificially imposed shear flow layer.

Gyrofluid model GEMR

The GEMR model consists of normalized equations for density (n_z), parallel velocity ($u_{z\parallel}$), parallel and perpendicular temperatures ($T_{z\parallel}$, $T_{z\perp}$), parallel and perpendicular components of the parallel heat flux ($q_{z\parallel}$, $q_{z\perp}$), electric potential (ϕ), and parallel magnetic potential ($A_\parallel$), where $z \in \{\mathrm{e},\mathrm{i}\}$ denotes the species (electrons and ions) [2, 3]. The model evolves the gradients as part of the dependent variables and includes a time-dependently self-consistent, circular toroidal magnetic equilibrium [4]. The implementation of a limiter allows for a separation between the closed field line region and the scrape-off-layer [5]. GEMR is based on field-aligned, unit-Jacobian coordinates (x,y,s), where x is a flux surface label, y represents a field line label, and s denotes the position along the magnetic field.

Implementation of RMPs and poloidal shear flow layers

RMPs are included in terms of a magnetic perturbation potential $A_\parallel^{\mathrm{P}}$. In order to satisfy the constraint of zero additional plasma current (note that RMPs are generated by external coil currents), the magnetic perturbation potential is obtained from the solution of Ampére's law

$$\nabla_\perp^2 A_\parallel^{\mathrm{P}} = \left[\frac{\partial}{\partial x} g^{xx} \frac{\partial}{\partial x} + g^{yy} \frac{\partial^2}{\partial y^2}\right] A_\parallel^{\mathrm{P}} = J_\parallel \stackrel{!}{=} 0 \tag{1}$$

subject to the boundary condition

$$A_\parallel^{\mathrm{P}}(x = x_1, x_9) = \sum_m (-1)^m A_0(x = x_1, x_9) \cos\left\{2\pi\left[ms - n\left(qs - y\right)\right]\right\} \tag{2}$$

where $g^{xx} = g^{xx}(x)$ and $g^{yy} = g^{yy}(x)$ are metric elements, m and n represent the poloidal and toroidal mode number, respectively, $q = m/n$ denotes the safety factor, and A_0 defines the amplitude of the perturbation potential at the radial boundaries x_1 and x_9. The sum in eq. 2 includes

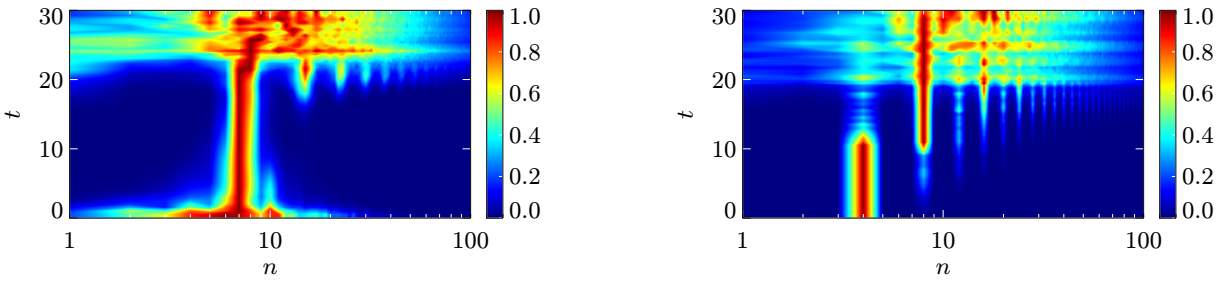

(a) $A_0 = 0$ (b) $A_0 = 1$

Figure 1: Toroidal mode number spectra of the advective electron heat transport $\langle Q_e \rangle_{xs}$ ($\langle \ldots \rangle_u$ denotes the average over u) for the unperturbed case (a) and for the case including an RMP with $n = 4$ (b). The heat flux amplitudes are time-dependently normalized to the maximum values.

all poloidal mode numbers in the considered radial range (cf. ref. [6]).

A shear flow layer is included in terms of a zonal electric potential, given by

$$\phi_{sh} = w_{sh} d_{sh}^2 \exp \frac{(x - x_{sh})^2}{2 d_{sh}^2} \tag{3}$$

where x_{sh} defines the radial position of the shear layer, w_{sh} denotes the maximum shear (located at $x = x_{sh}$), and d_{sh} determines the radial width of the shear layer (cf. ref. [7]).

Simulation setup

The simulation parameters are based on ASDEX-Upgrade-H-mode profiles characterized by the midpedestal values $n_e = n_i = 2.5 \cdot 10^{-19}\,\mathrm{m}^{-3}$, $T_e = 300\,\mathrm{eV}$, and $T_i = 360\,\mathrm{eV}$. [8]. The midpedestal values of the magnetic equilibrium field, the safety factor, and the magnetic shear are given by $B = 2\,\mathrm{T}$, $q = 4.5$, and $\hat{s} = 1.4$, respectively. The simulations are initialized by a turbulent bath of random density fluctuations (cf. ref. [3]).

Simulation results and discussion

At first, we investigate an H-mode scenario without imposed shear flow. We focus on the evolution of an ideal ballooning ELM blowout and omit to include sources for density and temperature. Without the action of RMPs, the prepared H-mode state evolves into an ideal ballooning instability with toroidal mode number $n = 7$. If we include a multiple RMP with $n = 4$, the mode number of the growing instability is shifted to a number which is resonant with the perturbation. Fig. 1 illustrates that the $E \times B$ advective electron heat transport transitions from $n = 7$ for $A_0 = 0$ to $n = (4, 8)$ for $A_0 = 1$. Considering the corresponding time traces shown in fig. 2a, we find that the RMP facilitates the growth of the instability. Both effects can be ascribed to the RMP induced formation of stationary density fluctuations which are larger than those of the initial turbulent bath. If we increase the amplitude of the turbulent bath, the transition from the most unstable mode ($n = 7$) to a resonant mode ($n = 4, 8$) is shifted to higher perturbation amplitudes. A mitigation of the ideal ballooning ELM by a nonlinear interaction between the most unstable mode and the modes imposed by the RMP is not observed.

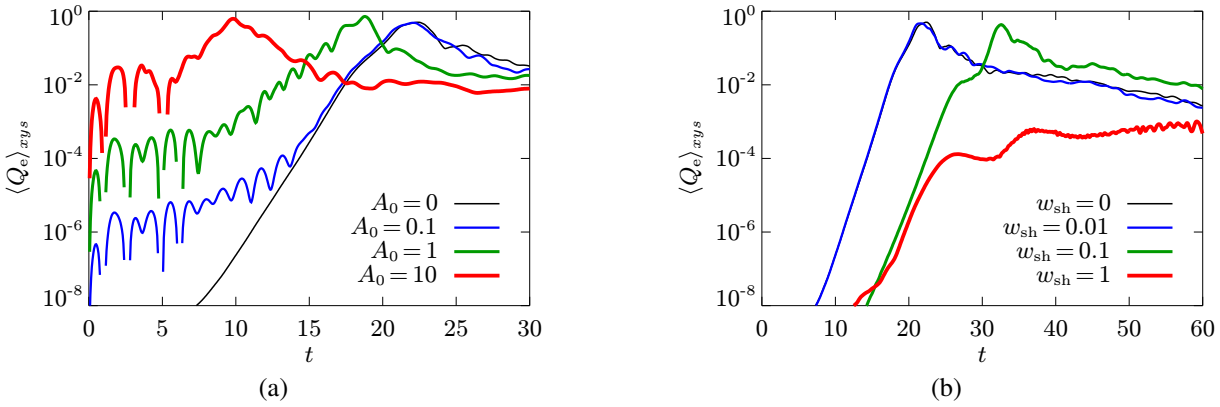

Figure 2: Advective electron heat transport dependence on the RMP amplitude (a), and the shear rate (b).

We now include an artificial shear flow layer located at the radial position of the steepest gradients. Fig. 2b shows that the shear flow delays or, if the shear rate exceeds a threshold value, suppresses the growth of the ideal ballooning instability.

In the following we discuss an H-mode scenario including both an artificially imposed shear flow layer as well as density and temperature sources. The shear flow counteracts the decrease and broadening of the density and temperature profiles. Thus, it allows to study the effects of RMPs on an H-mode-like state. Fig. 3 shows that the time trace of the unperturbed (i.e. no RMPs acting) advective electron heat transport exhibits periodic bursts. These bursts were found to be due to the intermittent formation of modes with the lowest mode numbers contained in the region around the shear flow layer (i.e. $n = 2$) (cf. ref. [7]). By increasing the RMP amplitude, an H-mode-like regime free of repetitive transport bursts is reached (cf. ref. [9]). Furthermore, the RMP involves a reduction of the fluctuation amplitudes. Fig. 4a illustrates that the effect on the time averaged electron density profiles is twofold: Low RMP amplitudes ($A_0 \sim 10$) increase the profile (due to a reduced transport associated with the reduction of the fluctuations), while high RMP amplitudes ($A_0 \sim 40$) lead to a decrease (due to an increased transport associated with the RMP induced formation of stationary convection cells). The time averaged potential profiles shown in fig. 4b exhibit a clear decrease if the RMP amplitude is increased. The hump around $x = 62.8$ reflects the artificially imposed Gaussian potential yielding the shear flow layer.

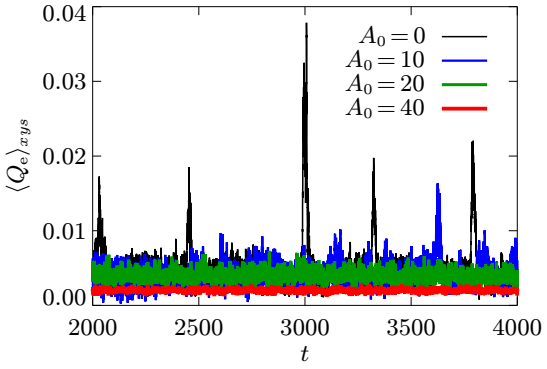

Figure 3: Advective electron heat transport dependence on the RMP amplitude.

We point out that the addition of the artificial zonal electric potential defined by eq. 3 involves the formation of a bidirectional shear flow layer which is not consistent with the unidirectional shear flow observed in the edge region of ASDEX Upgrade [10]. Nevertheless, the presented

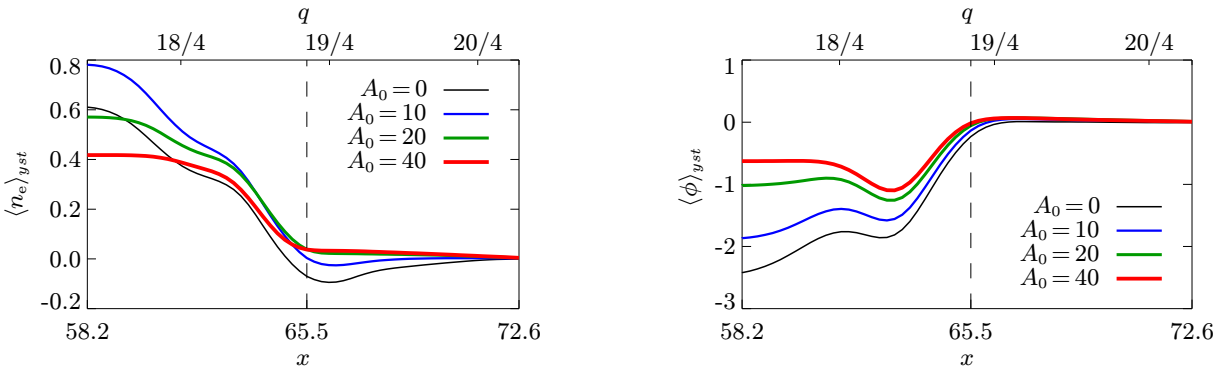

(a) n_e (b) ϕ

Figure 4: Electron density (a) and electric potential (b) dependence on the RMP amplitude.

approach is appropriate to study the interaction between RMPs and a localized (externally imposed) shear flow layer. The implementation of a more realistic, non-localized, unidirectional shear flow would involve far larger deviations from the self-consistently computed potential profile.

Acknowledgements

We thank B. D. Scott for providing the gyrofluid code GEMR. This work was supported by the Austrian Ministry of Science BMWF as part of the UniInfrastrukturprogramm of the Forschungsplattform Scientific Computing at LFU Innsbruck. Furthermore, the work was supported by the European Commission under the Contract of Association between EURATOM and ÖAW and was carried out within the framework of the European Fusion Development Agreement (EFDA). The views and opinions expressed herein do not necessarily reflect those of the European Commission.

References

[1] W. Suttrop et al., Phys. Rev. Lett. **106**, 225004 (2011)

[2] B. D. Scott, Phys. Plasmas **12**, 102307 (2005)

[3] A. Kendl et al., Phys. Plasmas **17**, 072302 (2010)

[4] B. D. Scott, Contrib. Plasma Phys. **46**, 714 (2006)

[5] T. T. Ribeiro and B. Scott, Plasma Phys. Control. Fusion **47**, 1657 (2005)

[6] D. Reiser and B. Scott, Phys. Plasmas **12**, 122308 (2005)

[7] P. Beyer et al., Plasma Phys. Control. Fusion **49**, 507 (2007)

[8] L. D. Horton et al., Nucl. Fusion **45**, 856 (2005)

[9] P. Beyer et al., Plasma Phys. Control. Fusion **53**, 054003 (2011)

[10] J. Schirmer et al., Nucl. Fusion **46**, S780 (2006)